YMTHE, Volume *31*

Supplemental Information

Genome editing with natural and engineered CjCas9 orthologs

Siqi Gao, Yao Wang, Tao Qi, Jingjing Wei, Ziying Hu, Jingtong Liu, Shuna Sun, Huihui Liu, and Yongming Wang

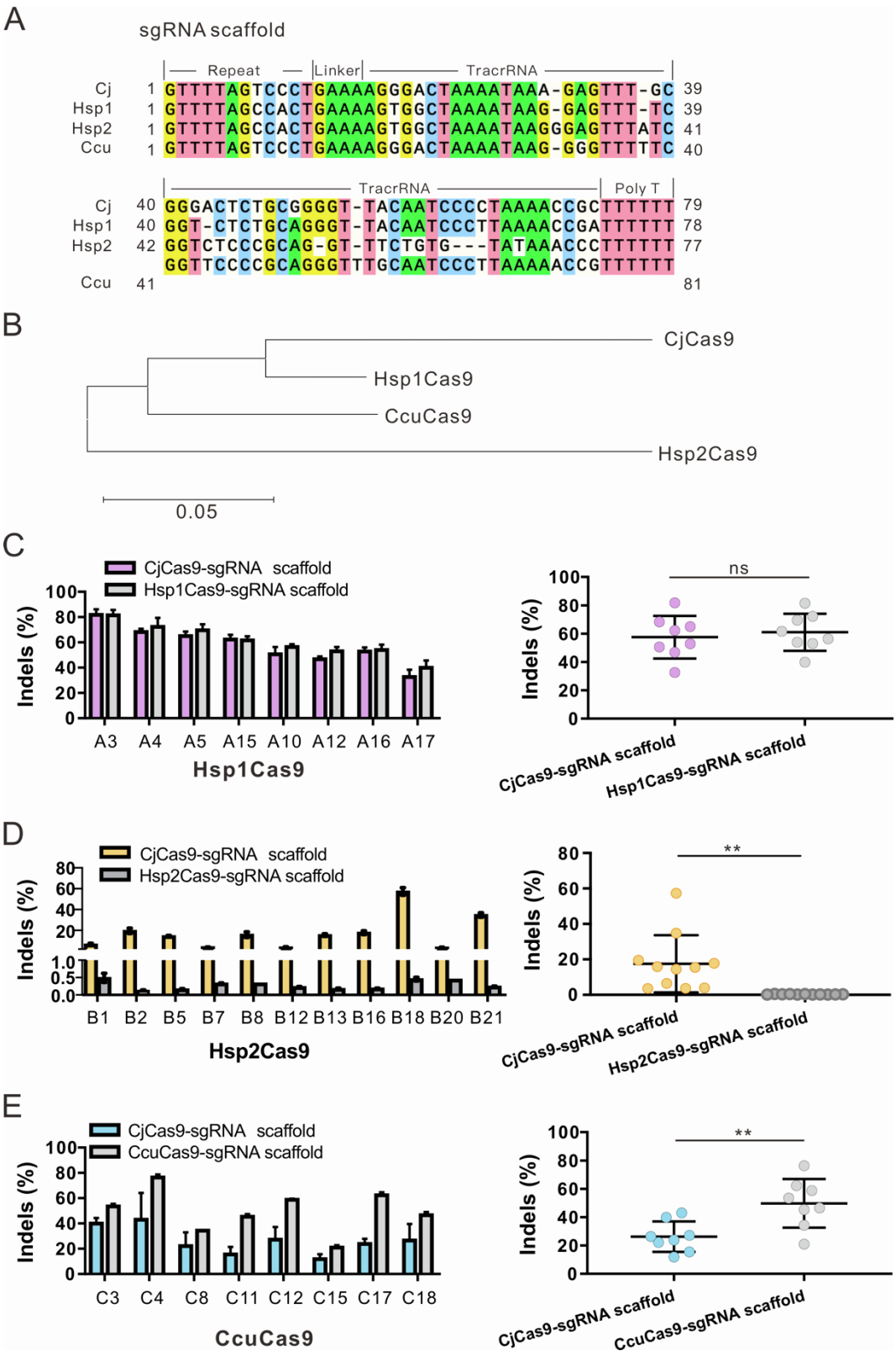

Figure S1. CjCas9 orthologs enable genome editing guided by their sgRNA scaffolds

(A) Comparison of the sgRNA scaffold sequences for CjCas9 orthologs. (B) The phylogenetic tree of the four sgRNA scaffolds. (C) The editing efficiencies of

Hsp1Cas9 with the CjCas9-sgRNA scaffold or Hsp1Cas9-sgRNA scaffold in HEK293T cells. (D) The editing efficiencies of Hsp2Cas9 with the CjCas9-sgRNA scaffold or Hsp2Cas9-sgRNA scaffold in HEK293T cells. (E) The editing efficiencies of CcuCas9 with the CjCas9-sgRNA scaffold or CcuCas9-sgRNA scaffold in HEK293T cells. Cells were treated with puromycin. The data represent the mean ± SD; n=3. Student's t-test, $^{**}p < 0.01$. Indel efficiencies were determined by targeted deep sequencing.

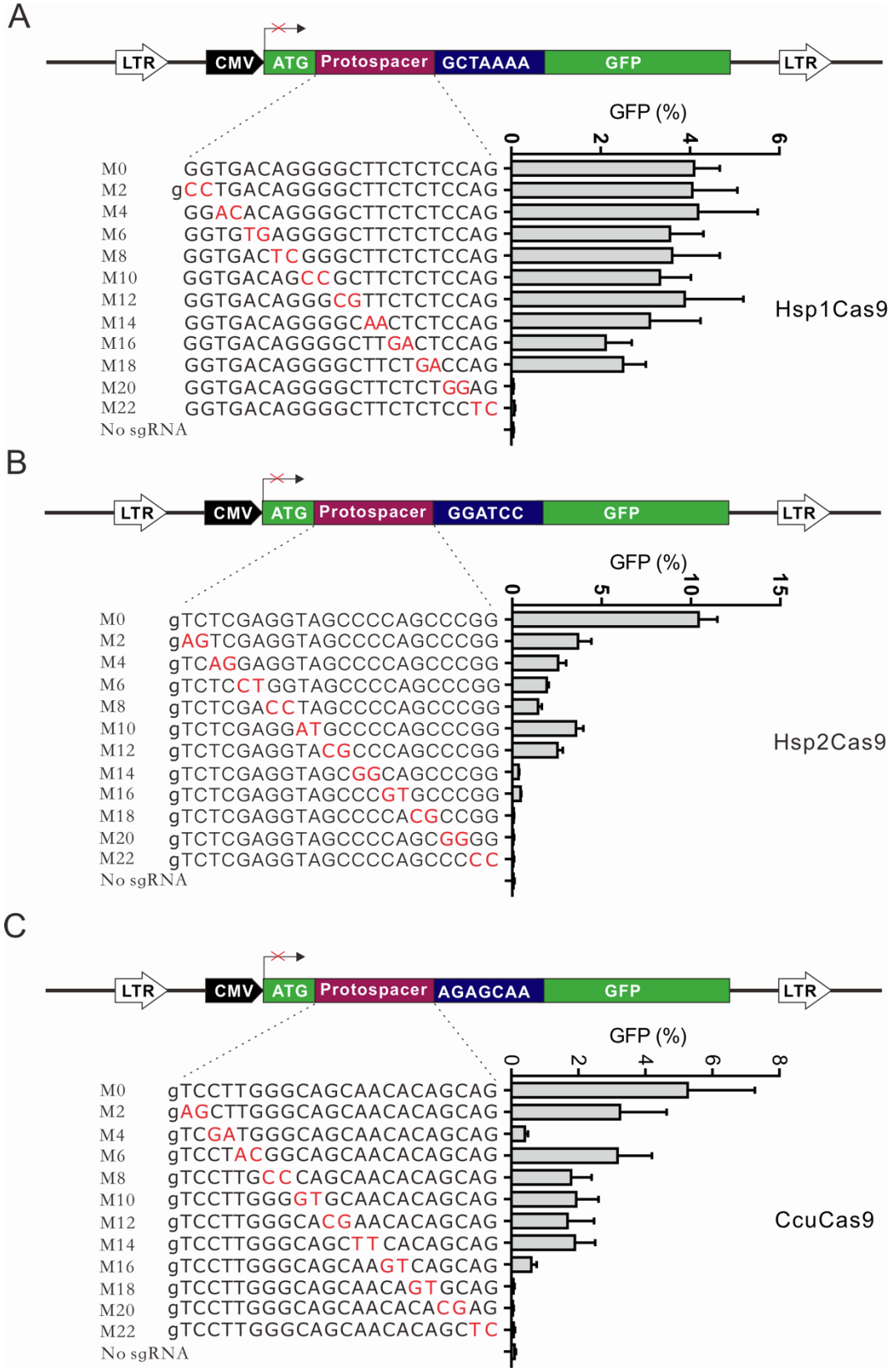

Figure S2. Analysis of specificity for (A) Hsp1Cas9, (B) Hsp2Cas9, and (C) CcuCas9 by the GFP-activation assay. Schematics of the GFP-activation reporters are shown on the top. A target sequence with the corresponding PAM is

inserted between ATG and GFP coding sequence, disrupting GFP expression. Cas9s were transfected with sgRNAs with CjCas9-sgRNA scaffold. Genome editing induced GFP expression. A panel of sgRNAs with dinucleotide mutations (red bases) is shown below. An additional G at the 5' terminal is added for U6 promoter transcription. The sgRNA activities were measured by the proportion of GFP-positive cells. The data represent the mean ± SD; n=3.

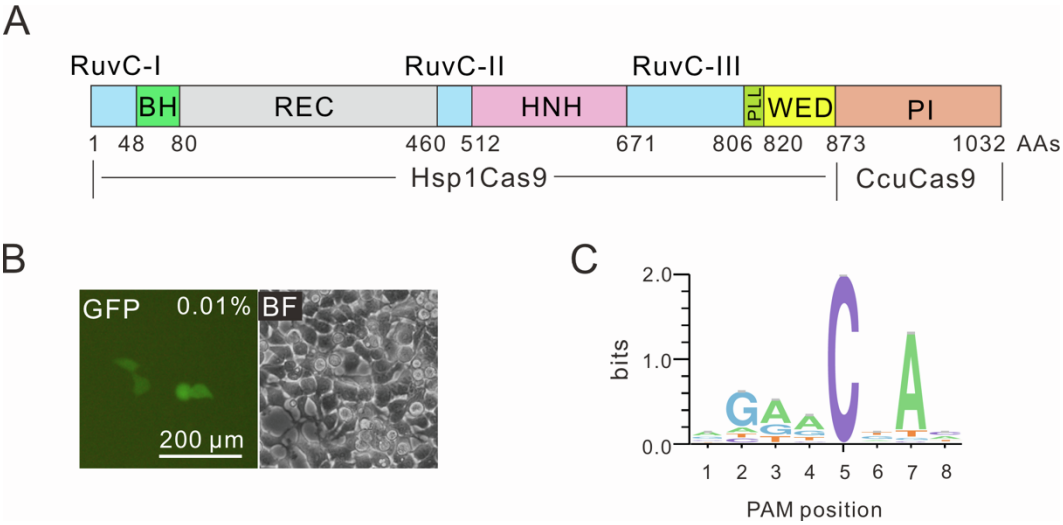

Figure S3. Generation of chimeric Hsp1-CcuCas9

(A) Schematic diagram of chimeric Hsp1-CcuCas9 nuclease. The Hsp1Cas9 PI domain was replaced with the CcuCas9 PI domain. (B) GFP-activation assay revealed that Hsp1-CcuCas9 induced GFP expression. The proportion of GFP-positive cells is shown. BF, bright field; GFP, green fluorescent protein. (C) WebLogo for Hsp1-CcuCas9 is generated based on deep sequencing data.

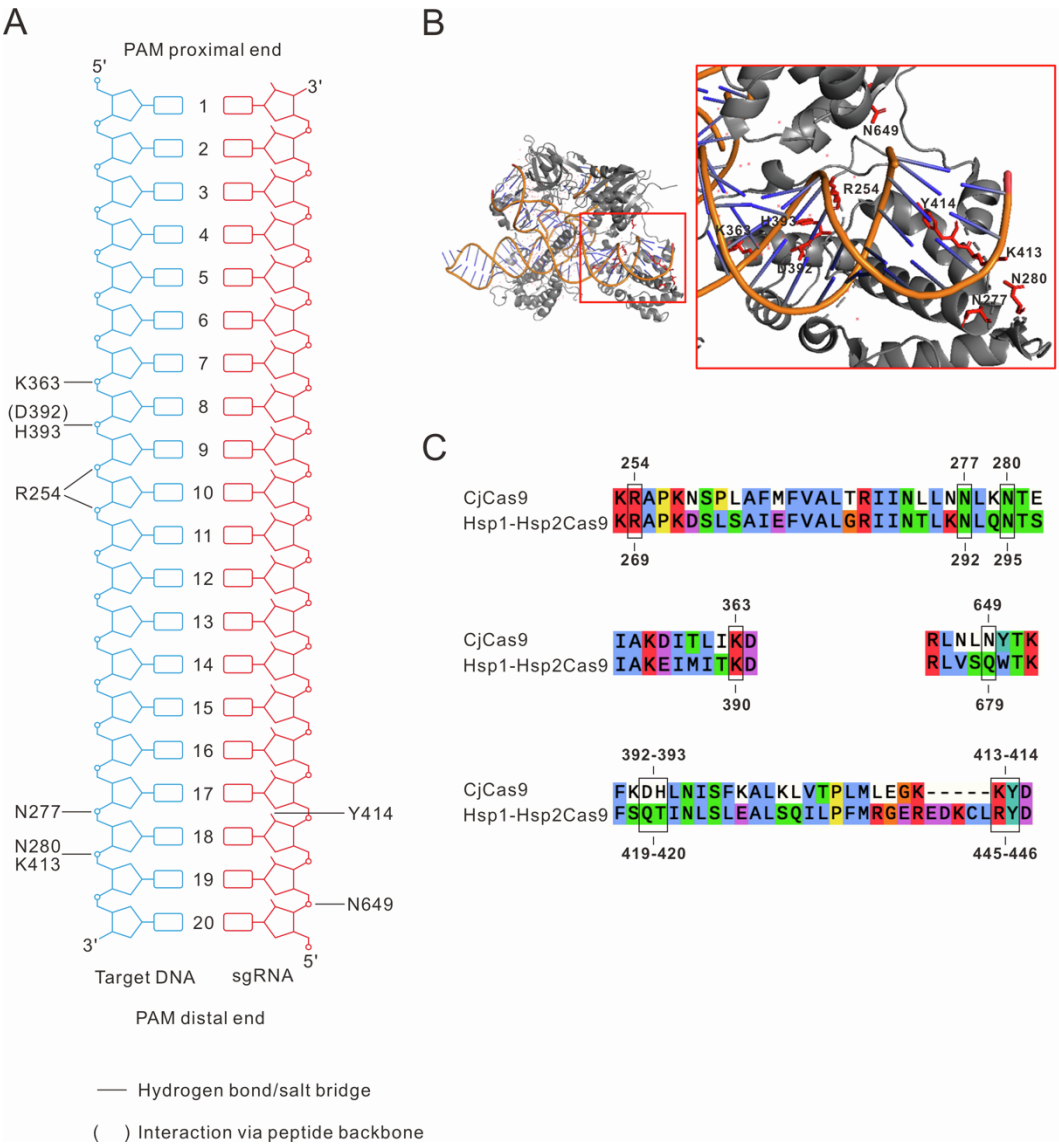

Figure S4. Engineering of Hsp1-Hsp2Cas9 variants based on CjCas9 crystal structure

(A) Schematic depicting interactions of CjCas9 residues with the target DNA-sgRNA duplex, based on PDB accession 5X2H and 5X2G [1]. (B) The crystal structure of the CjCas9 interacting with the target DNA-sgRNA duplex (SMTL ID: 5x2g.1.A). The nine residues that form hydrogen bonds at the target DNA-sgRNA interface are shown. (C) Alignment of CjCas9 and Hsp1-Hsp2Cas9 protein sequences. Black boxes indicate equivalent residues of CjCas9 and Hsp1-Hsp2Cas9 interacting with the target DNA-sgRNA duplex. The positions of the residues are shown.

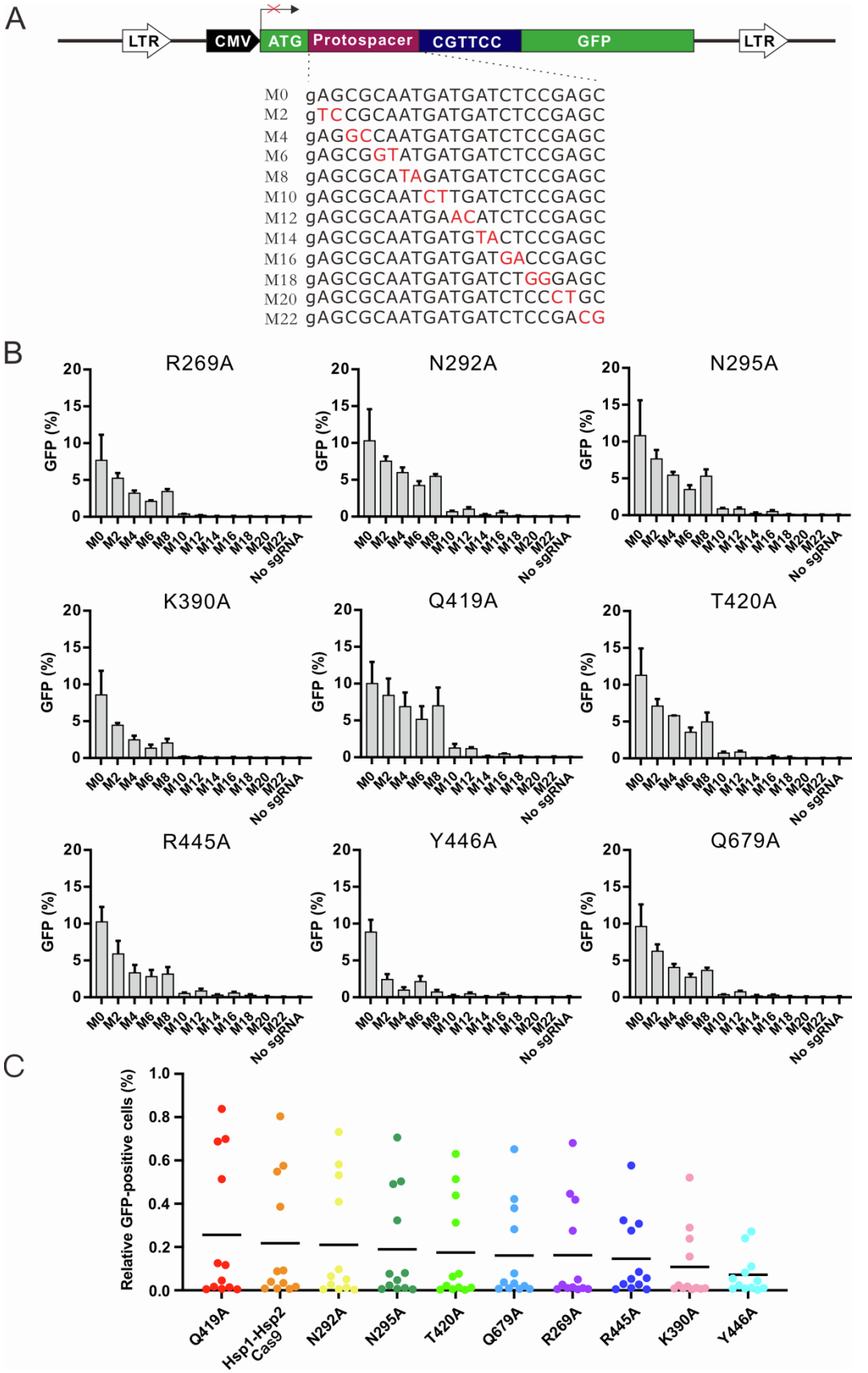

Figure S5. Specificity analysis of Hsp1-Hsp2Cas9 variants

(A) Schematic of the GFP-activation assay showing the specificity of the nucleases

in HEK293T cells on the top. Cas9s were transfected with sgRNAs with CjCas9-sgRNA scaffold. A panel of sgRNAs with dinucleotide mutations (red bases) is shown below. An additional G is added at the 5' end of sgRNA for U6 promoter transcription. (B) Specificity of single-mutation Hsp1-Hsp2Cas9 variants analyzed by the GFP-activation assay. The activity of each sgRNA of the Hsp1-Hsp2Cas9 variants was measured by the proportion of GFP-positive cells. The data represent the mean ± SD; n=3. (C) Quantification of off-target editing efficiency based on GFP-activation assay. The off-target editing efficiency is normalized by on-target editing efficiency.

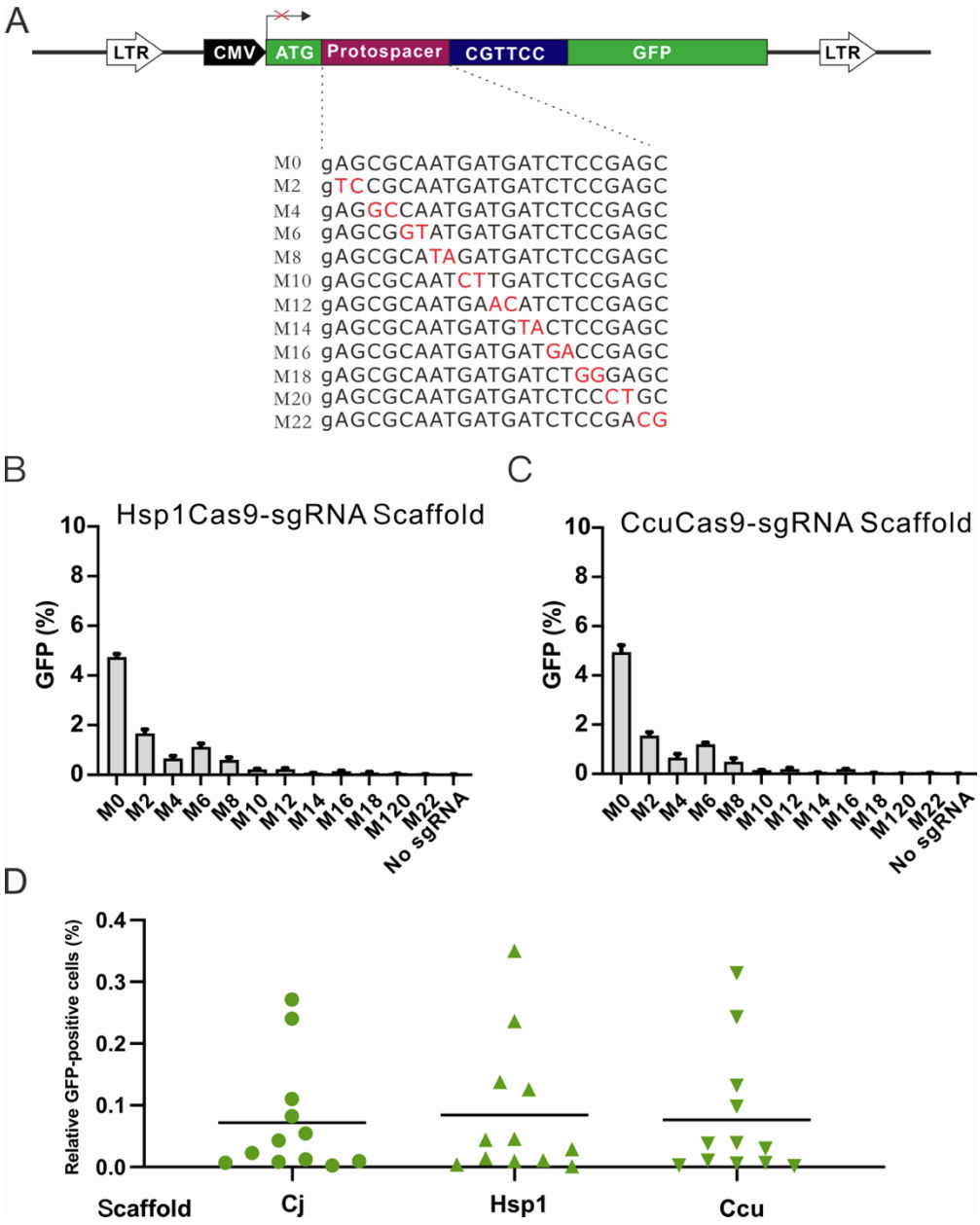

Figure S6. Specificity analysis of Hsp1-Hsp2Cas9-Y with different scaffolds

(A) Schematic of the GFP-activation assay showing the specificity of the nucleases in HEK293T cells on the top. A panel of sgRNAs with dinucleotide mutations (red bases) is shown below. An additional G is added at the 5' end of sgRNA for U6 promoter transcription. (B) Specificity of Hsp1-Hsp2Cas9-Y analyzed by the GFP-activation assay with sgRNAs with Hsp1Cas9-sgRNA scaffold. The data represent the mean ± SD; n=3. (C) Specificity of Hsp1-Hsp2Cas9-Y analyzed by the GFP-activation assay with sgRNAs with CcuCas9-sgRNA scaffold. The data represent the mean ± SD; n=3. (D) Quantification of off-target editing efficiency based on GFP-activation assay. The off-target editing efficiency is normalized by on-target editing efficiency.

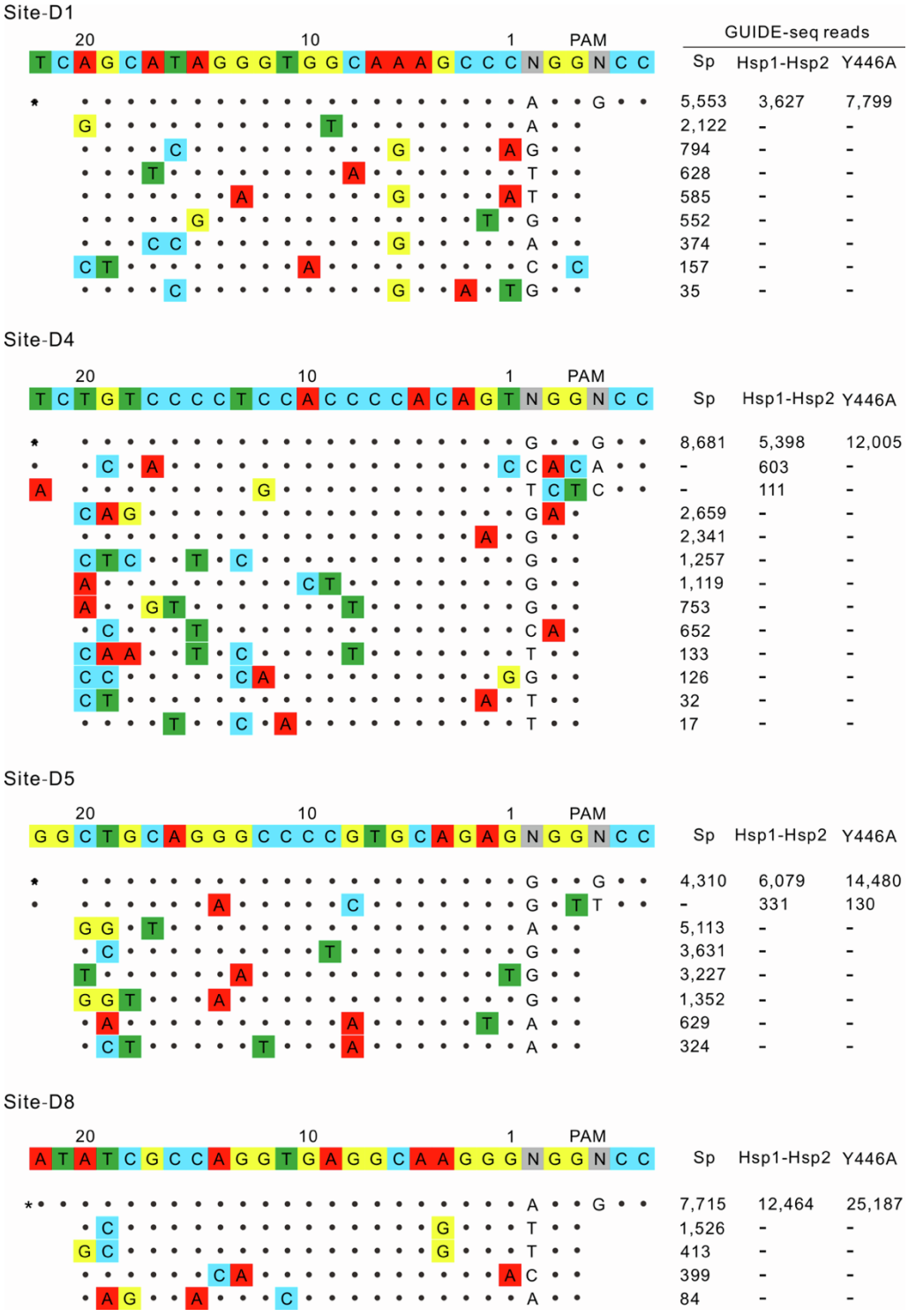

Figure S7. Genome-wide specificities of SpCas9, Hsp1-Hsp2Cas9 and Hsp1-Hsp2Cas9-Y determined by GUIDE-seq

The on-target site is marked with "*". Mismatched bases within off-target sites are shown and highlighted in color. Read counts for on-target and off-target sites are listed on the right. Sp, SpCas9; Hsp1-Hsp2, Hsp1-Hsp2Cas9; Y446A, Hsp1-Hsp2Cas9-Y. SpCas9 was transfected with sgRNAs with the SpCas9-sgRNA scaffold. Hsp1-Hsp2Cas9 and Hsp1-Hsp2Cas9-Y were transfected with sgRNAs with the CjCas9-sgRNA scaffold.

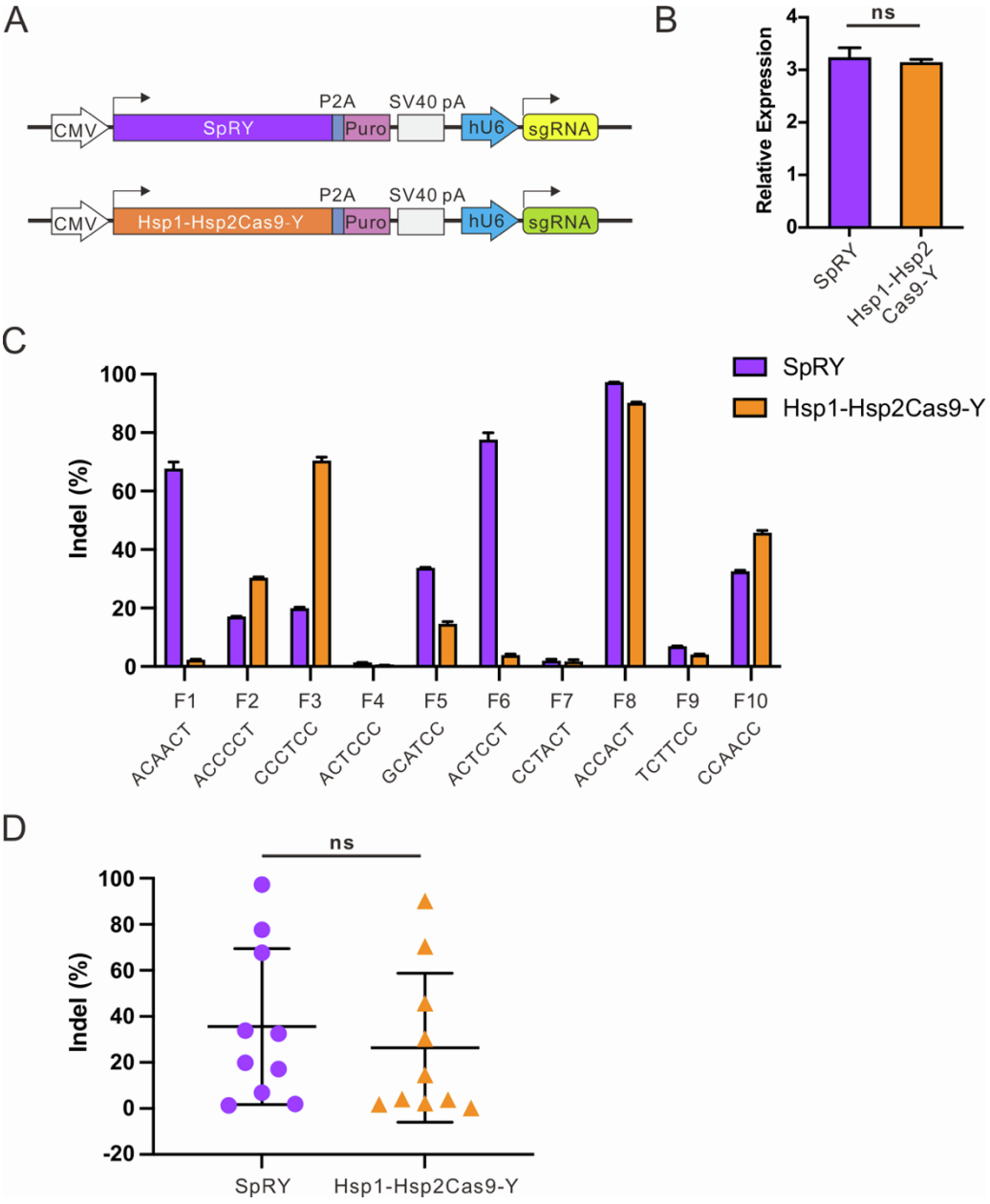

Figure S8. Comparison of genome editing activity between SpRY and Hsp1-Hsp2Cas9-Y

(A) Schematic of the Cas9 nuclease and sgRNA-expressing plasmid constructs. pA, polyA; Puro, puromycin resistant gene; hU6, human U6 promoter. SpRY was transfected with sgRNAs with the SpCas9-sgRNA scaffold. Hsp1-Hsp2Cas9-Y was transfected with sgRNAs with the CjCas9-sgRNA scaffold. (B) Expression levels of SpRY and Hsp1-Hsp2Cas9-Y relative to *GAPDH* were measured by RT-qPCR. (C) Comparison of SpRY and Hsp1-Hsp2Cas9-Y genome editing activity at ten endogenous sites with the N_4CY PAM in HEK293T cells. Cells were treated with puromycin. Indel efficiencies were determined by targeted deep sequencing. The data represent the mean ± SD; n=3. (D) Quantification of the editing efficiencies of SpRY and Hsp1-Hsp2Cas9-Y. The data represent the mean ± SD.

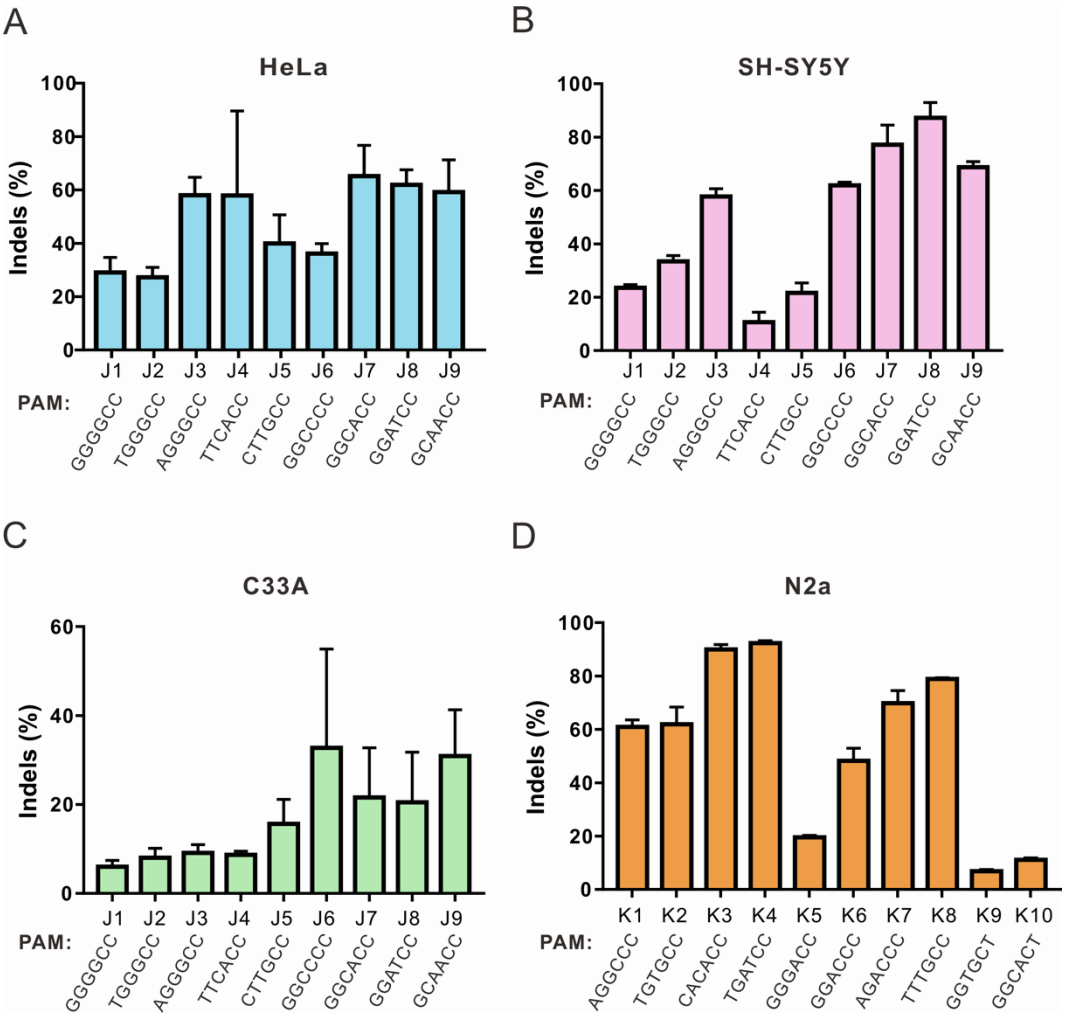

Figure S9. Hsp1-Hsp2Cas9-Y enables genome editing in diverse cell types
Hsp1-Hsp2Cas9-Y enables genome editing in diverse cell types, including (A) HeLa, (B) SH-SY5Y, (C) C33A, and (D) N2a cells. The PAM sequences are shown below. Hsp1-Hsp2Cas9-Y was transfected with sgRNAs with the CjCas9-sgRNA scaffold. Cells were treated with puromycin. Indel efficiencies were determined by targeted deep sequencing. The data represent the mean ± SD; n=3.

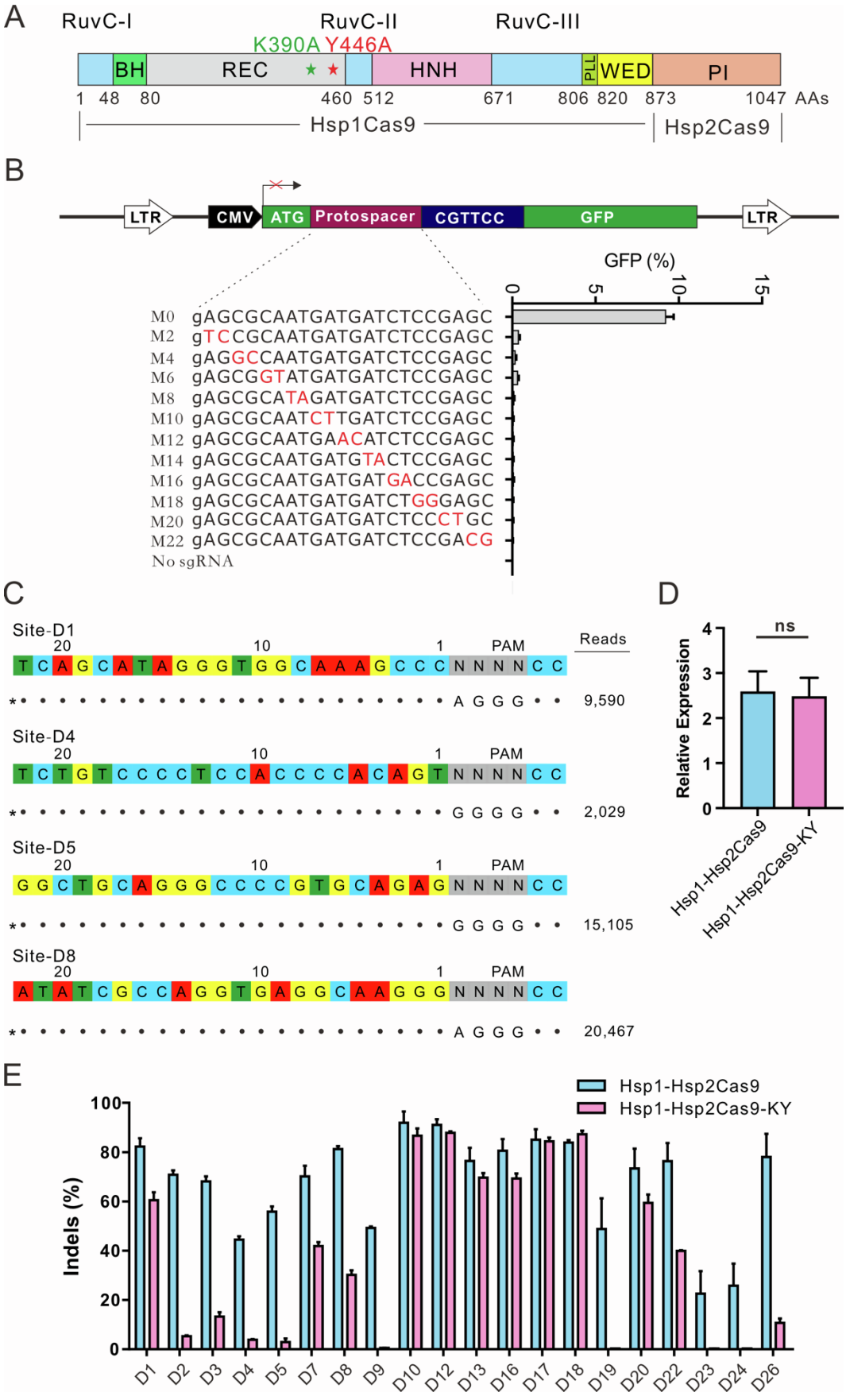

Figure S10. Characterization of Hsp1-Hsp2Cas9-KY for Genome editing

(A) Schematic diagram of chimeric Hsp1-Hsp2Cas9-KY nuclease. It contains K390A and Y446A mutations. (B) The specificity of Hsp1-Hsp2Cas9-KY is evaluated by the GFP-activation assay. Hsp1-Hsp2Cas9-KY was transfected with sgRNAs with the CjCas9-sgRNA scaffold. A panel of sgRNAs with dinucleotide mutations (red bases) is shown below. An additional G at the 5' terminal is added for U6 promoter transcription. The data represent the mean ± SD; n=3. (C) Genome-wide specificities of Hsp1-Hsp2Cas9-KY determined by GUIDE-seq. Hsp1-Hsp2Cas9-KY was transfected with sgRNAs with the CjCas9-sgRNA scaffold. The on-target site is marked with "*". Read counts are listed on the right. (D) Expression levels of Hsp1-Hsp2Cas9 and Hsp1-Hsp2Cas9-KY relative to *GAPDH* were measured by RT-qPCR. (E) Comparison of Hsp1-Hsp2Cas9 and Hsp1-Hsp2Cas9-KY genome editing activity at 20 endogenous sites with the N_4CC PAM in HEK293T cells. Hsp1-Hsp2Cas9 and Hsp1-Hsp2Cas9-KY were transfected with sgRNAs with the CjCas9-sgRNA scaffold. Cells were treated with puromycin. The data represent the mean ± SD; n=3.

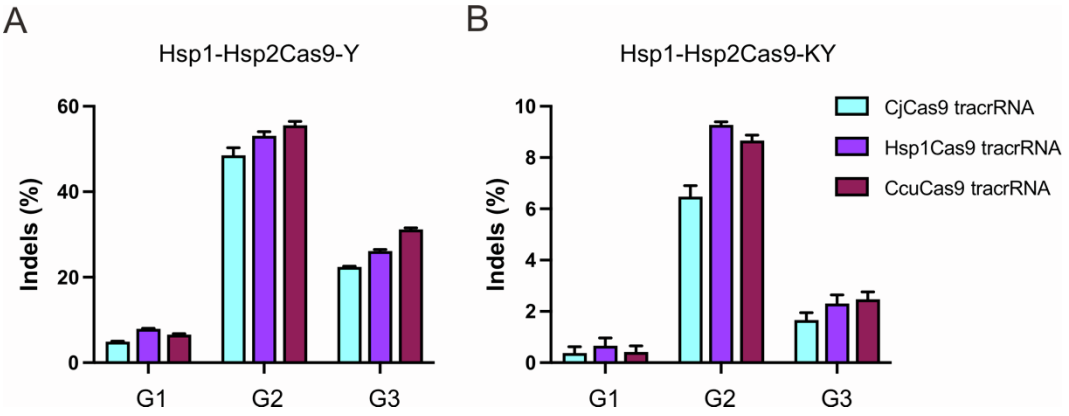

Figure S11. Test of genome editing activity of Hsp1-Hsp2Cas9-Y and Hsp1-Hsp2Cas9-KY with different sgRNA scaffolds

(A) Genome editing ability of Hsp1-Hsp2Cas9-Y with different scaffolds measured by targeted deep sequencing. Cells were treated with puromycin. The data represent the mean ± SD; n=3. (B) Genome editing ability of Hsp1-Hsp2Cas9-KY with different scaffolds measured by targeted deep sequencing. The data represent the mean ± SD; n=3.

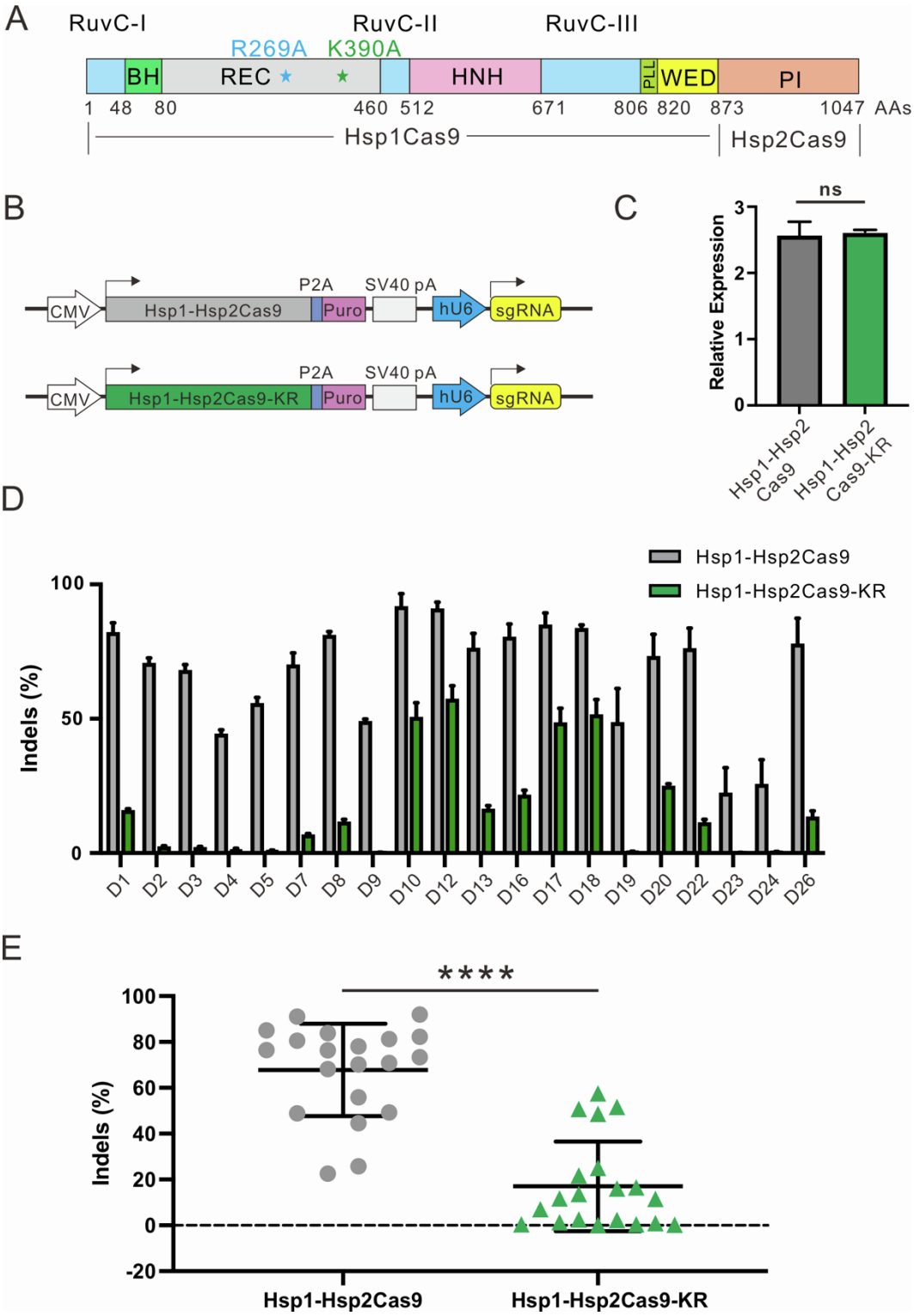

Figure S12. Comparison of genome editing activity between Hsp1-Hsp2Cas9 and Hsp1-Hsp2Cas9-KR

(A) Schematic diagram of chimeric Hsp1-Hsp2Cas9-KR nuclease. It contains K390A and R269A mutations. (B) Schematic of plasmid constructs of the Cas9 nuclease and sgRNA with CjCas9-sgRNA scaffold. pA, polyA; Puro, puromycin resistant gene; hU6, human U6 promoter. Both Cas9 were transfected with sgRNAs

with the CjCas9-sgRNA scaffold. (C) Expression levels of Hsp1-Hsp2Cas9-Y and Hsp1-Hsp2Cas9-KY relative to *GAPDH* were measured by RT-qPCR. (D) Comparison of Hsp1-Hsp2Cas9 and Hsp1-Hsp2Cas9-KR genome editing activity at 20 endogenous sites with the N_4CC PAM in HEK293T cells. Cells were treated with puromycin. The data represent the mean ± SD; n=3. (E) Quantification of the editing efficiencies of Hsp1-Hsp2Cas9 and Hsp1-Hsp2Cas9-KY. Indel efficiencies were determined by targeted deep sequencing. The data represent the mean ± SD.

REFERENCES

1. Yamada, M., Watanabe, Y., Gootenberg, J.S., Hirano, H., Ran, F.A., Nakane, T., Ishitani, R., Zhang, F., Nishimasu, H., and Nureki, O. (2017). Crystal Structure of the Minimal Cas9 from Campylobacter jejuni Reveals the Molecular Diversity in the CRISPR-Cas9 Systems. Mol Cell *65*, 1109-1121 e1103. 10.1016/j.molcel.2017.02.007.

Table S1. Summary of the type II-A and type II-C Cas9 orthologs

Type	Cas9	PAM	Size (aa)	Activity	Specificity	Reference
Type II-A	SpCas9	NGG	1368	High	Low	Jinek et al. (2012)
Type II-A	SaCas9	NNGRRT	1053	High	Medium	Ran et al. (2015)
Type II-A	ScCas9	NNG	1380	Medium	Low	Chatterjee et al. (2018)
Type II-A	SlugCas9	NNGG	1054	High	Medium	Hu et al. (2021)
Type II-A	SauriCas9	NNGG	1061	High	Medium	Hu et al. (2020)
Type II-A	SchCas9	NNGR	1054	Medium	High	Wang et al. (2022)
Type II-A	St1Cas9	NNRGAA	1121	Medium	Medium	Agudelo et al. (2020)
Type II-C	NmeCas9	NNNNGATT	1082	Medium	High	Amrani et al. (2018)
Type II-C	Nme2Cas9	NNNNCC	1082	Medium	High	Edraki et al. (2019)
Type II-C	CjCas9	NNNNRYAC	984	Medium	High	Kim et al. (2017)
Type II-C	Nsp2Cas9	NNNNCC	1067	Medium	High	Wei et al. (2022)
Type II-C	BlatCas9	NNNNCNAA	1092	Medium	High	Gao et al. (2020)

The following tables are submitted in Excel format

Table S2. DNA sequences of plasmids were used in this study

Table S3. The human codon-optimized Cas9 sequences

Table S5. Primers used in this study

Table S6. All data in this study

Table S7. The information of raw sequencing data

Table S4. Target sites used in this study

	Name	Gene	Target_Seq	PAM	Description
Figure3B	A1	VEGFA	ggtgacaggggcttctctccag	GCTAAAA	Endogenous target site of human
	A2	GRIN2B	gtgacaaggggaataaagccaa	CCTGAAA	Endogenous target site of human
	A3	VEGFA	ccgattcaagtggggaatggca	AGCAAAA	Endogenous target site of human
	A4	VEGFA	gggcaaggggttggtaactgag	GGTAAAA	Endogenous target site of human
	A5	VEGFA	tcagttcgaggaaagggaaagg	GGCAAAA	Endogenous target site of human
	A6	EMX1	gaggagcctataaacaattgtg	ACTAAAA	Endogenous target site of human
	A7	GRIN2B	cagtattcagtgctgcagaagg	TCAAGAA	Endogenous target site of human
	A8	EMX1	aaagactgagagaaacatgagg	ACAGAAA	Endogenous target site of human
	A9	EMX1	caagagaataggtcctaagagg	AGTGAAA	Endogenous target site of human
	A10	GRIN2B	cagtcagctctgtgctgtgagg	GGGAAAA	Endogenous target site of human
	A11	GRIN2B	tttggaagaaaaggtcacaaga	TATGAAA	Endogenous target site of human
	A12	GRIN2B	aggatggggtagaatggcactg	AGGAAAA	Endogenous target site of human
	A13	VEGFA	actgagggtaaaaagacctggg	GTAGGAA	Endogenous target site of human
	A14	VEGFA	ggctggggagctcgaaatgcag	GAGGAAA	Endogenous target site of human
	A15	VEGFA	tggggcttgctgggaacctggg	CTGGGAA	Endogenous target site of human
	A16	GRIN2B	gaggtgacaaggggggaaagga	GTGGGAA	Endogenous target site of human
	A17	GRIN2B	ggtgacagcagcaatgagaatg	TATAGAA	Endogenous target site of human
Figure3C	B1	AAVS1	cgcaccattctcacaaagggag	TTTTCC	Endogenous target site of human
	B2	AAVS1	agggaggagagatgcccggaga	GGACCC	Endogenous target site of human
	B3	GRIN2B	gatggtgtagacctgtgaagcg	TGGTCC	Endogenous target site of human
	B4	GRIN2B	aaagggagtgatggatgaagag	GGATCC	Endogenous target site of human
	B5	AAVS1	aggactgcatgggtcagcacag	GCTGCC	Endogenous target site of human
	B6	GRIN2B	aagggagtgatggatgaagagg	GATCCC	Endogenous target site of human
	B7	AAVS1	aagcctgagcgcctctcctggg	CTTGCC	Endogenous target site of human
	B8	AAVS1	tggtgcagcgccgagaaggaag	TGCTCC	Endogenous target site of human
	B9	GRIN2B	aatatcaagccactctaaatag	ACTACC	Endogenous target site of human
	B10	GRIN2B	gtagcttctctctccttccagg	TCTGCC	Endogenous target site of human
	B11	VEGFA	atcttaagtgtatgcttcgtgg	ACTTCC	Endogenous target site of human
	B12	VEGFA	ccgggaccctccactcctcctg	GGCCCC	Endogenous target site of human
	B13	VEGFA	agggggggtgccgaggaccgaag	GGCACC	Endogenous target site of human
	B14	VEGFA	atgtctatcagcgcagctactg	CCATCC	Endogenous target site of human
	B15	VEGFA	gagagaggggctcctgacacag	GCATCC	Endogenous target site of human
	B16	VEGFA	tctcgaggtagccccagcccgg	GGATCC	Endogenous target site of human
	B17	VEGFA	tggaagggacaatgccttctgg	GTCTCC	Endogenous target site of human
	B18	VEGFA	tggaggtagagcagcaaggcaa	GGCTCC	Endogenous target site of human
	B19	VEGFA	ccgaggctccgggaacacgcgg	CCGGCC	Endogenous target site of human
	B20	GRIN2B	tttacaatgagagacaatactg	GCATCC	Endogenous target site of human
	B21	EMX1	ctccagcctgggcgatacaggg	AGATCC	Endogenous target site of human
	B22	VEGFA	tagcagcgaccccgtccatgg	CTTTCC	Endogenous target site of human
Figure3D	C1	AAVS1	cgcaccattctcacaaagggag	TTTTCAA	Endogenous target site of human
	C2	VEGFA	gacggacagacagacagacacc	GCCCCCA	Endogenous target site of human
	C3	AAVS1	tccttgggcagcaacacagcag	AGAGCAA	Endogenous target site of human
	C4	AAVS1	agggaggagagatgcccggaga	GGACCCA	Endogenous target site of human
	C5	VEGFA	ccggcggcggacagtggacgcg	GCGGCGA	Endogenous target site of human
	C6	VEGFA	tgggaccactgaggacagaaag	AGAGCAA	Endogenous target site of human
	C7	VEGFA	gggagcacacacgtacactcca	ACAACCA	Endogenous target site of human
	C8	AAVS1	tgagaatggtgcgtcctaggtg	TTCACCA	Endogenous target site of human
	C9	VEGFA	ctgttcccaaagtgttaccccc	CTCCCTA	Endogenous target site of human
	C10	VEGFA	aggcggcggtgtgcgcagacag	TGCTCCA	Endogenous target site of human
	C11	VEGFA	tctccagaccctacctctgccc	AGTGCTA	Endogenous target site of human
	C12	VEGFA	tctcgaggtagccccagcccgg	GGATCCA	Endogenous target site of human
	C13	VEGFA	gcagcaaggcaaggctccaatg	CACCCAA	Endogenous target site of human
	C14	VEGFA	aggggacggaaatttcataccc	CTTCCAA	Endogenous target site of human
	C15	VEGFA	caaccctggaccagcaatgcca	CCACCAA	Endogenous target site of human
	C16	VEGFA	cgggaccctccactcctcctgg	GCCCCAA	Endogenous target site of human
	C17	VEGFA	gtgagagagtgagagagagaca	CGGGCCA	Endogenous target site of human
	C18	TIMM8B	tatgtagtccaaggtcatgtag	CCAGCAA	Endogenous target site of human
	C19	VEGFA	agaatatgcccaccactcctgg	ACTGCTA	Endogenous target site of human
	C20	VEGFA	ctggaaagagcagaagaaaaag	GCAACAA	Endogenous target site of human
	C21	TIMM8B	gtgggaggaagagggtgctcgg	ATGACCA	Endogenous target site of human
	C22	VEGFA	cacatagcgggaagctggacgg	GGGCCAA	Endogenous target site of human
	C23	LINC01588	ttggagtgtgtttggatgagga	GGGACAA	Endogenous target site of human
	C24	VEGFA	ccaggaggatgagagccaggga	AGGACCA	Endogenous target site of human
	C25	VEGFA	ggagggggagaagggaccagag	AGGGCAA	Endogenous target site of human
Figure4D	D1	AAVS1	tcagcatagggtggcaaagccc	AGGGCC	Endogenous target site of human
	D2	AAVS1	gcagcgcaaagtgacaatggcc	AGGGCC	Endogenous target site of human
	D3	AAVS1	ctctgacctgcattctctcccc	TGGGCC	Endogenous target site of human
	D4	AAVS1	tctgtcccctccaccccacagt	GGGGCC	Endogenous target site of human
	D5	AAVS1	ggctgcagggccccgtgcagag	GGGGCC	Endogenous target site of human
	D6	AAVS1	cggcggggtcgagctcggcgcc	GGGGCC	Endogenous target site of human
	D7	AAVS1	cttcctccaccctgcatagccc	TGGGCC	Endogenous target site of human
	D8	AAVS1	atatcgccaggtgaggcaaggg	AGGGCC	Endogenous target site of human
	D9	AAVS1	gaatcatgtcccaccgcatgga	TGGGCC	Endogenous target site of human
	D10	AAVS1	agggaggagagatgcccggaga	GGACCC	Endogenous target site of human
	D11	AAVS1	gggtctgagggaggaggggctg	GGGGCC	Endogenous target site of human
	D12	AAVS1	tgagaatggtgcgtcctaggtg	TTCACC	Endogenous target site of human
	D13	AAVS1	aagcctgagcgcctctcctggg	CTTGCC	Endogenous target site of human
	D14	AAVS1	gttccttttccttctccttct	GGGGCC	Endogenous target site of human
	D15	AAVS1	atgctgtcctgaagtggacata	GGGGCC	Endogenous target site of human

	D16	VEGFA	ccgggaccctccactcctcctg	GGCCCC	Endogenous target site of human
	D17	VEGFA	agggggggtgccgaggaccgaag	GGCACC	Endogenous target site of human
	D18	VEGFA	tctcgaggtagccccagcccgg	GGATCC	Endogenous target site of human
	D19	VEGFA	aggaaacgacctgggaccacct	GTTCCC	Endogenous target site of human
	D20	VEGFA	ctgtcccctcctgagcccatgg	GCAACC	Endogenous target site of human
	D21	AAVS1	gtccaggccaagtaggtggcct	GGGGCC	Endogenous target site of human
	D22	VEGFA	aagggtgagtctcaggccacag	GGACCC	Endogenous target site of human
	D23	EMX1	aatgtggtgcttgagaagtgga	TGGCCC	Endogenous target site of human
	D24	GRIN2B	cccatcaagctgggctccaagg	AGGGCC	Endogenous target site of human
	D25	AAVS1	tgggtttgagagaggaggggct	GGGGCC	Endogenous target site of human
	D26	GRIN2B	tttacaatgagagacaatactg	GCATCC	Endogenous target site of human
Figure4E	E1	AAVS1	gccgtctctctcctgagtccgg	ACCACT	Endogenous target site of human
	E2	AAVS1	cccctggaagatgccatgacag	GGGGCT	Endogenous target site of human
	E3	AAVS1	gtggctaaagccagggagacgg	GGTACT	Endogenous target site of human
	E4	AAVS1	agaagactagctgagctctcgg	ACCCCT	Endogenous target site of human
	E5	AAVS1	gtggaccctgaacccacgcgg	AATCCT	Endogenous target site of human
	E6	AAVS1	tatcaggagactaggaaggagg	AGGCCT	Endogenous target site of human
	E7	AAVS1	ctgggaaacctagtgagaaccc	ATCTCT	Endogenous target site of human
	E8	VEGFA	tctccagaccctacctctgccc	AGTGCT	Endogenous target site of human
	E9	EMX1	tgcggtgacagagcaagtgctg	GGGGCT	Endogenous target site of human
	E10	VEGFA	aaagcgacaggggcaaagtgag	TGACCT	Endogenous target site of human
	E11	EMX1	gcagggcagtgcggggacaccg	GGGGCT	Endogenous target site of human
	E12	VEGFA	gagtcctcacgaaactgagggt	GAACCT	Endogenous target site of human
	E13	GRIN2B	gtgaagggtagtaagatatatg	AGACCT	Endogenous target site of human
	E14	GRIN2B	aacagagttagctgcaatccag	TGGTCT	Endogenous target site of human
	E15	VEGFA	gctgacatgacaaataccaggg	TGAGCT	Endogenous target site of human
	E16	EMX1	ctgagacaagacaggagcccag	CAAGCT	Endogenous target site of human
Figure6B	sg1	B4GALNT2	tgtgacgccttcgggcatcagg	AAAGCT	Target site of BeGALNT2 exon3
	sg2	B4GALNT2	agctataacttggaggatgcct	ACGACC	Target site of BeGALNT2 exon3
	sg3	B4GALNT2	ggatgcctacgacccgcgtgac	CTCCCC	Target site of BeGALNT2 exon3
	sg4	B4GALNT2	acccgcgtgacctccccgcagt	GAACCT	Target site of BeGALNT2 exon3
	sg1	CMAH	aagaaaatggagttttgcttct	AGAACT	Target site of CMAH exon3
	sg2	CMAH	tgcttctagaactaaatcctcc	TAACCC	Target site of CMAH exon3
	sg3	CMAH	taacccgtgggattcagaaccc	AGATCT	Target site of CMAH exon3
	sg4	CMAH	agaacccagatctcctgaagat	TTGGCT	Target site of CMAH exon3
Figure6D	H1	EMX1	gtagctgggactacaggcatgc	ACCACC	Endogenous target site of human
	H2	EMX1	agtgtctaggggggcctgtagga	ACCCCT	Endogenous target site of human
	H3	EMX1	gggactacaggcatgcaccacc	ACACCT	Endogenous target site of human
	H4	EMX1	tgtctaggggggcctgtaggaac	CCCTCC	Endogenous target site of human
	H5	EMX1	agccattttcctaatatgatgg	GCATCC	Endogenous target site of human
	H6	EMX1	caaaataattggcccagggctc	ACCACT	Endogenous target site of human
	H7	EMX1	tcgacctcctgggctcgagaga	TCTTCC	Endogenous target site of human
	H8	EMX1	tgtctagcctcatgtgttctgc	TCACCT	Endogenous target site of human
	H9	EMX1	tggccttggggcgtcaggaggc	CCAACC	Endogenous target site of human
	H10	EMX1	gaacacatgaggctagacaggt	ACAACT	Endogenous target site of human
	H11	AAVS1	ccccttcttgtaggcctgcatc	ATCACC	Endogenous target site of human
	H12	AAVS1	ccactgagcactgaaggcctgg	CCGGCC	Endogenous target site of human
	H13	EMX1	tcagtgttccaataaagttcaa	ACTCCT	Endogenous target site of human
	H14	EMX1	ataagatctctgttttcccttc	ACTCCC	Endogenous target site of human
Figure S8C	F1	EMX1	gaacacatgaggctagacaggt	ACAACT	Endogenous target site of human
	F2	EMX1	agtgtctaggggggcctgtagga	ACCCCT	Endogenous target site of human
	F3	EMX1	tgtctaggggggcctgtaggaac	CCCTCC	Endogenous target site of human
	F4	EMX1	ataagatctctgttttcccttc	ACTCCC	Endogenous target site of human
	F5	EMX1	agccattttcctaatatgatgg	GCATCC	Endogenous target site of human
	F6	EMX1	caccacatatgttatctcattt	ACTCCT	Endogenous target site of human
	F7	EMX1	agcagttaatatttatcaaaag	CCTACT	Endogenous target site of human
	F8	EMX1	caaaataattggcccagggctc	ACCACT	Endogenous target site of human
	F9	EMX1	tcgacctcctgggctcgagaga	TCTTCC	Endogenous target site of human
	F10	EMX1	tggccttggggcgtcaggaggc	CCAACC	Endogenous target site of human
Figure S9A-C	J1	AAVS1	gtgaactggagtgtgacagcct	GGGGCC	Endogenous target site of human
	J2	AAVS1	cttcctccaccctgcatagccc	TGGGCC	Endogenous target site of human
	J3	AAVS1	atatcgccaggtgaggcaaggg	AGGGCC	Endogenous target site of human
	J4	AAVS1	tgagaatggtgcgtcctaggtg	TTCACC	Endogenous target site of human
	J5	AAVS1	aagcctgagcgcctctcctggg	CTTGCC	Endogenous target site of human
	J6	VEGFA	ccgggaccctccactcctcctg	GGCCCC	Endogenous target site of human
	J7	VEGFA	agggggggtgccgaggaccgaag	GGCACC	Endogenous target site of human
	J8	VEGFA	tctcgaggtagccccagcccgg	GGATCCA	Endogenous target site of human
	J9	VEGFA	ctgtcccctcctgagcccatgg	GCAACC	Endogenous target site of human
Figure S9D	K1	mEMX1	ggtgggaaggtgagctaagcag	AGGCCC	Endogenous target site of Mouse
	K2	mEMX1	taggatggtttcatgccgggga	TGTGCC	Endogenous target site of Mouse
	K3	mEMX1	ccggctctgacggtgcacccgg	CACACC	Endogenous target site of Mouse
	K4	mTh	gtggtcttgggagagagcccca	TGATCC	Endogenous target site of Mouse
	K5	mTh	gagtaggacttaggaagccaca	GGGACC	Endogenous target site of Mouse
	K6	mTh	actaggacgttcctagaaccca	GGACCC	Endogenous target site of Mouse
	K7	mRNF2	aggccagcttggaactacatag	AGACCC	Endogenous target site of Mouse
	K8	mRNF2	aagaagccaaggatgcaagtcg	TTTGCC	Endogenous target site of Mouse
	K9	mEMX1	gatccgggacccctggaagacag	GGTGCT	Endogenous target site of Mouse
	K10	mTh	atgcagctaagaagtatgaagg	GGCACT	Endogenous target site of Mouse
Figure S9D	G1	AAVS1	ccaccaacgccgacggtatcag	CGCCCT	Endogenous target site of human
	G2	AAVS1	ccccttcttgtaggcctgcatc	ATCACC	Endogenous target site of human
	G3	AAVS1	ccactgagcactgaaggcctgg	CCGGCC	Endogenous target site of human